The Role of CHPD and AIMI processing on enhancing J_C and connectivity of *in-situ* MgB_2 strand

F. Wan[1], M.D. Sumption[1], M.A. Rindfleisch[2],& E.W. Collings[1]

1.Center for Superconducting & Magnetic Materials (CSMM), Department of Materials Science & Engineering, The Ohio State University Columbus, OH 43210, U.S.A.

2. Hyper Tech Research, Inc. Columbus, OH 43212, U.S.A.

CEC/ICMC SAVE THE DATE JULY 21-25, 2019 CONNECTICUT CONVENTION CENTER, HARTFORD CT

Abstract

Research into in-situ MgB_2 strand has been focused on improvements in J_C through reduction of porosity. In a high-performance superconducting strand the nature of the mechanism of reduced porosity and how to best manipulate it to elucidate enhancements in J_c is an area of ongoing investigation. Both of cold-high-pressure-densification (CHPD) and advanced-internal-magnesium-infiltration (AIMI) methods can effectively remove the voids in the in-situ MgB_2 strands. This study shows the nature of the reduced porosity for *in-situ* MgB_2 strands lies on generating better connections between MgB_2 grains. The CHPD method applying bi-axially 1.0 GPa and 1.5 GPa yielded 4.2 K $J_{CM||}$ values of about 9.6×10^4 A/cm^2 and 8.5×10^4 A/cm^2 at 5 T, respectively, as compared the 6.0×10^4 A/cm^2 of typical *in-situ* MgB_2 strand. Moreover, AIMI-processed monofilamentary MgB_2 strand obtained even higher $J_{CM||}$

Introduction

First, the presence of voids in the powder-in-tube *in-situ* MgB_2 strands induces anisotropic connectivity and thus results in the differences between $J_{CM\perp}$ and $J_{CM||}$. The influence of intrinsic and extrinsic properties for *in-situ* MgB_2 strands in terms of $J_{CM\perp}$ and $J_{CM||}$ were investigated.

Second, the dominate pinning centers in MgB_2 are grain boundaries. Grain connectivity, K of MgB_2 superconductor can be estimated by normalizing the maximum flux pinning force with that of fully-connected MgB_2 bulk. The relationship between porosity and grain connectivity for the *in-situ* MgB_2 strand was also discussed in this study.

Experimental Details

PIT *in-situ* and AIMI MgB_2 strands were provided by Hyper-Tech Research of Columbus, OH. Strand composition was designed to be 2.0 mol% C based on B. The AIMI strands were heat-treated at 625ºC and16h . The PIT *in-situ* strands were bi-axially densified with 1.0 and 1.5 GPa at room temperature and then were heat-treated at 675ºC/1h.

Transport critical current testing was performed in pool boiling Helium in transverse magnetic fields up to 13 T. The transport J_Cs (J_{CT}s) were calculated by normalizing transport critical currents with the area of MgB_2 core.

Magnetization versus perpendicular ($\perp$) and parallel ($||$) magnetic field loops were measured by using a Quantum Design Model 6000 PPMS. The values of magnetic J_Cs (J_{CM}s) were extracted from the full height ΔM of the MH loops together with using the standard Bean Model expressions. Flux pinning forces were obtained through $J_{CM} \times B$.

Electron optics of the transverse cross sections for the MgB_2 strands were performed with an Apreo Scanning Electron Microscope (SEM).

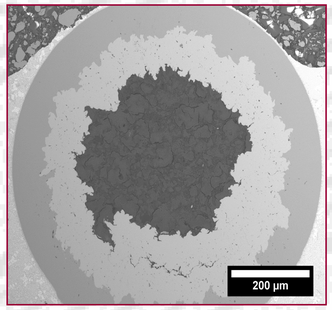

Figure 1. BSE-SEM image of P00 (PIT *in-situ* MgB_2 wire with 2.0 mol% C doping).

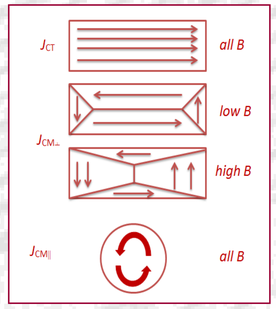

Figure 2. "Rooftop" critical state profiles

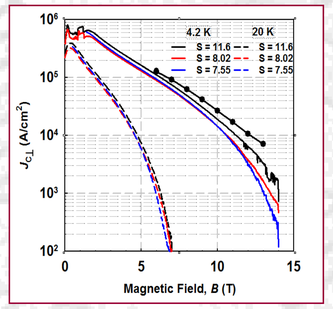

Figure 3. J_c *vs.* transverse *B* for strand P00 with varied aspect ratio (S = Length/diameter)

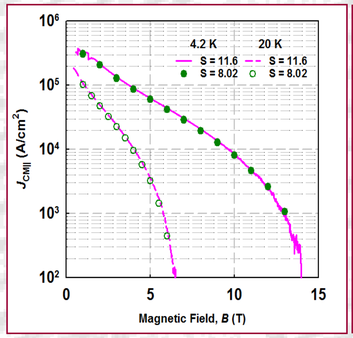

Figure 4. J_c *vs.* longitudinal *B* for strand P00 with varied aspect ratio S

$J_{CM\perp}$s agrees with J_{CT} at low fields, whereas the bifurcation of $J_{CM\perp}$s and J_{CT} happened at high fields. Moreover, $J_{CM\perp}$s were greatly affected by the aspect ratio S = length/diameter for PIT *in-situ* MgB_2 strand, especially at high fields. The values of $J_{CM\perp}$ is determined by the extrinsic properties as well as the intrinsic properties of *in-situ* MgB_2 strands.

Whereas, $J_{CM||}$s were independent on the aspect ratio S; therefore, the values of $J_{CM||}$ were only determined by the intrinsic properties of the *in-situ* MgB_2 strands.

We can investigate the role of CHPD and AIMI technique on enhancing the current-carrying-capacity of the *in-situ* MgB_2 strands by comparing the $J_{CM||}$s.

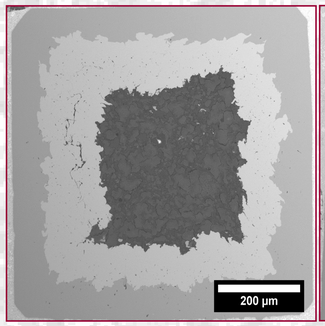

Figure 5. BSE-SEM image of P10 (PIT *in-situ* MgB_2 wire with 2.0 mol% C doping and cold-densified with 1.0 GPa).

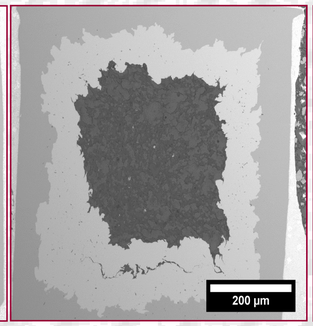

Figure 6. BSE-SEM image of P15 (PIT *in-situ* MgB_2 wire with 2.0 mol% C doping and cold-densified with 1.5 GPa)

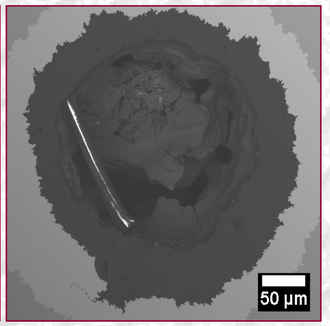

Figure 7. BSE-SEM image of A00 (AIMI MgB_2 strand with 2.0 mol% C doping).

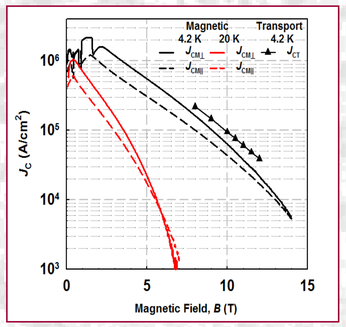

Figure 8. J_{CT}, $J_{CM\perp}$, and $J_{CM||}$ versus *B* at 4.2 and 20 K for AIMI strand A00.

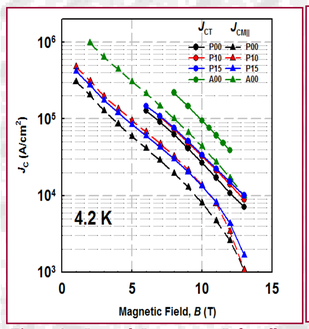

Figure 9. J_{CT} and $J_{CM\perp}$ versus *B* for all *in-situ* MgB_2 strands at 4.2 K.

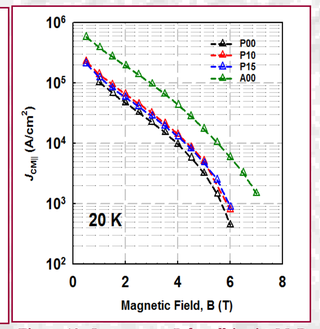

Figure 10. $J_{CM||}$ versus *B* for all *in-situ* MgB_2 strands at 20 K.

The CHPD technique significantly enhanced $J_{CM||}$ of PIT *in-situ* strands at 4.2 K. J_{CT}s were slightly enhanced by the CHPD technique. The increases in J_{CT} and $J_{CM||}$ indicated that the both longitudinal and transverse connections between MgB_2 fibers were enhanced.

Whereas, as the porosity of the *in-situ* MgB_2 strand is reduced by the CHPD technique, the transverse connections between MgB_2 fibers were more effectively enhanced than the longitudinal connections.

With the formation of a high density MgB_2 layer, the AIMI strand A00 attained the highest J_{CT} and $J_{CM||}$

Strand Name	J_{CT}, 4.2K 10T (X10^4 A/cm^2)	$J_{CM\perp}$, 4.2K 5 T (X10^4 A/cm^2)	$J_{CM||}$, 20 K 5 T (X10^3 A/cm^2)	$F_{p,max||}$, 4.2 K (GN/m^3)	$F_{p,max||}$, 20 K (GN/m^3)
P00	2.7	5.9	3.2	4.3	1.1
P10	3.2	9.6	5.1	6.3	1.4
P15	3.4	8.5	4.8	5.6	1.3
A00	9.4	30.8	17.2	19.6	4.1

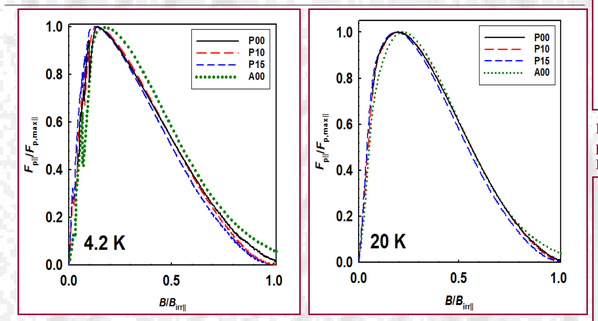

Figure 11. $F_{pi}/F_{p,max||}$ versus $B/B_{irr||}$ for all strands at 4.2 K and 20 K.

It can be seen that the peak pinning occurred at b = $B/B_{irr||}$ close to 0.2 at 4.2 and 20 K, which is in agreement with the Dew-Hughes/Kramer model. In other words, the dominant pinning centers for the strands P00, P10, P15, and A00 are grain boundaries.

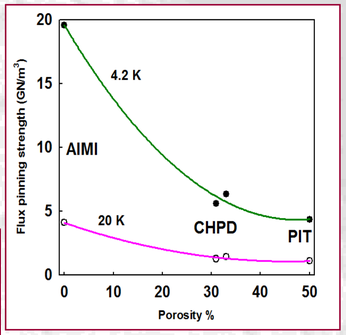

Figure 12. Schematic diagram of parallel flux pinning force density versus porosity for *in-situ* MgB_2 strands.

Fully-connected MgB_2, where grain connectivity K = 1, estimably can obtain the flux pinning density of 90 GN/m^3 and 22 GN/m^3 [1].

Strand P00 has the transverse grain connectivity $K_{||}$ of 0.05. The $K_{||}$s of the CHPD-processed strands, P10 and P15 were enhanced to 0.06. The AIMI-processed strand, A00 has the $K_{||}$ of 0.20.

Conclusions

- $J_{CM||}$s is merely determined by the intrinsic properties of *in-situ* MgB_2 strands, so the current-carrying capacity of *in-situ* MgB_2 strands can be represented by $J_{CM||}$as well as J_{CT}.
- The CHPD of 1.0 GPa and 1.5 GPa enhanced the 4.2 K, 5 T $J_{CM||}$ from 6.0×10^4 A/cm^2 to 9.6×10^4 A/cm^2 and 8.5×10^4 A/cm^2, respectively.
- AIMI strand attained the highest J_{CT} and $J_{CM||}$ at 4.2 and 20 K due to the formation of a high dense MgB_2 layer.
- By eliminating the voids through CHPD technique and AIMI technique, better connections between MgB_2 grains can be obtained in *in-situ* MgB_2 strands.

Acknowledgements

This work was supported by the NIH grant 4R44EB006652-02.

Reference

[1] T. Matsushita, M. Kiuchi, A. Yamamoto, J. Shimoyama, and K. Kishio, "Critical current density and flux pinning in superconducting MgB_2," Physica C, 468 (2008) 1833.